Mass Spectrometric Analysis Reveals an Increase in Plasma Membrane Polyunsaturated Phospholipid Species upon Cellular Cholesterol Loading†

Titta S. Blom,‡,§ Mirkka Koivusalo,‡,|| Esa Kuismanen,⊥ Risto Kostiainen,# Pentti Somerharju,|| and Elina Ikonen*,§

Department of Molecular Medicine, National Public Health Institute, and Department of Medical Chemistry, Institute of Biomedicine, Department of Biosciences, Division of Biochemistry, and Department of Pharmacy, Viikki Drug Discovery Technology Center, University of Helsinki, Helsinki, Finland

Received August 10, 2001; Revised Manuscript Received October 5, 2001

ABSTRACT: Here we used electrospray ionization mass spectrometry for quantitative determination of lipid molecular species in human fibroblasts and their plasma membrane incorporated into enveloped viruses. Both influenza virus selecting ordered domains and vesicular stomatitis virus (VSV) depleted of such domains [Scheiffele, P., et al. (1999) *J. Biol. Chem. 274*, 2038−2044] were analyzed. The major difference between influenza and VSV was found to be a marked enrichment of glycosphingolipids in the former. The effect of chronic cholesterol loading on viral lipid composition was studied in Niemann−Pick type C (NPC) fibroblasts. Both NPC-derived influenza and VSV virions contained increased amounts of cholesterol. Furthermore, polyunsaturated phosphatidylcholine, phosphatidylethanolamine, and phosphatidylserine were enriched in NPC-derived virions at the expense of the monounsaturated ones. When normal fibroblasts were acutely loaded with cholesterol using cyclodextrin complexes, an adjustment toward increasingly unsaturated phospholipid species was observed, most clearly for phosphatidylcholine and sphingomyelin. Our results provide evidence that (1) glycosphingolipids are enriched in domains through which influenza virus buds, (2) chronic cholesterol accumulation increases the cholesterol content of both glycosphingolipid-enriched and intervening plasma membrane domains, and (3) an increase in membrane cholesterol content is accompanied by an increased level of polyunsaturated species of the major membrane phospholipids. We suggest that remodeling of phospholipids toward higher unsaturation may serve as both an acute and a long-term adaptive mechanism in human cellular membranes against cholesterol excess.

During recent years, interest in the role of lipids in molecular membrane biology has rapidly increased. This is largely due to the emerging notion that membrane lipids can regulate diverse cellular processes such as signal transduction, membrane trafficking, and membrane−cytoskeleton interactions. However, the actual lipid composition of the membrane regions involved in these processes is not known. These analyses are complicated by the fact that, in the two major lipid categories, glycerophospholipids and sphingolipids, hundreds of individual structures are possible due to the large number of different headgroups and the varying length and unsaturation of the hydrophobic tails. In addition, highly purified biological membranes can usually be obtained only in minute quantities, and therefore, traditional techniques based on thin-layer or column chromatography are inadequate for the determination of a detailed lipid composition.

Cholesterol is an essential constituent in the membranes of higher eukaryotes, and its concentration and cellular distribution are tightly regulated (*1*). Cholesterol modulates the physical properties of phospholipids in the bilayer, and its level seems to be intimately coupled to those of other lipids by mechanisms that are only partially understood. The cholesterol content of cellular membranes is known to modulate those of choline-containing phospholipids. For example, cholesterol loading enhances the biosynthesis of phosphatidylcholine (*2*) but inhibits that of sphingomyelin (*3*). In addition, cholesterol affects fatty acid saturation by regulating the biosynthesis of monounsaturated fatty acids via stearoyl-CoA desaturase (*4*).

An important aspect of lipid interactions in biological membranes is the formation of domains, i.e., localized regions with distinct lipid composition. For instance, domains enriched in cholesterol and sphingolipids, termed rafts, are found in the plasma membrane as well as in internal cellular membranes (*5*−*8*). The actual lipid and protein composition of such domains has not been established, but this information is going to be crucial for understanding the physical

† This research was supported by the Academy of Finland (Grants 43184 and 43668 to E.I. and Grant 39584 to P.S.), the Ara Parseghian Medical Research Foundation (to E.I.), and The Sigrid Juselius Foundation (to P.S. and E.I.).

* Correspondence should be addressed to this author at the Department of Molecular Medicine, National Public Health Institute, Biomedicum Helsinki, P.O. Box 104, 00251 Helsinki, Finland. Tel: +358-9-4744 8469. Fax: +358-9-4744 8960. E-mail: elina.ikonen@ktl.fi.

‡ These authors contributed equally to this work.

§ Department of Molecular Medicine, National Public Health Institute.

|| Department of Medical Chemistry, Institute of Biomedicine, University of Helsinki.

⊥ Department of Biosciences, Division of Biochemistry, University of Helsinki.

Department of Pharmacy, Viikki Drug Discovery Technology Center, University of Helsinki.

10.1021/bi0156714 CCC: $20.00
Published on Web 11/08/2001

principles underlying the assembly of rafts and raft-dependent cellular functions. It is well established that enveloped viruses budding from the plasma membrane select specialized membrane regions for budding and can be obtained essentially free of cellular contaminants. Moreover, evidence has been provided that influenza virus buds from ordered, raft-like plasma membrane domains while vesicular stomatitis virus (VSV)[1] incorporates more fluid, raft-depleted domains to its envelope (*9*).

In this work, we have carried out a compositional lipid analysis of plasma membrane samples incorporated into influenza and vesicular stomatitis viruses. This was achieved by using the recently developed electrospray ionization mass spectrometry (ESI-MS) method. This method allows the analysis of individual molecular species at the low picomole level (*10*). Moreover, quantitative data can be obtained by using internal standards (*10, 11*). To investigate the effect of chronically increased amount of cholesterol on the levels of other plasma membrane lipids, we also isolated the viruses from the fibroblasts of a patient suffering from the severe cholesterol deposition disorder Niemann−Pick type C disease (NPC). In addition, the effect of acute cholesterol loading on the lipid composition of normal fibroblasts was determined. The most important results were that (i) cholesterol loading caused a significant increase of polyunsaturated species at the expense of monounsaturated ones in several phospholipid classes, (ii) the cholesterol content of both raft- and non-raft-like plasma membrane domains of NPC cells was higher than in controls, and (iii) the lipid composition of influenza and VSV was closely similar with the exception that glycosphingolipids were more abundant in the former. We discuss the implications of these findings on the regulation of membrane fluidity and on the cellular pathology of NPC as well as on the organization of rafts.

EXPERIMENTAL PROCEDURES

Materials. Methyl-β-cyclodextrin and phospholipase D from *Streptomyces* species (type VII) were obtained from Sigma. The acyl-coenzyme A:cholesterol acyltransferase (ACAT) inhibitor PKF 058-035 was a generous gift from Novartis. Silver Xpress kit was from Novex (The Netherlands), and fluorescamine was from Molecular Probes Inc. (Eugene, OR). Synthetic phospholipid standards were obtained from Avanti Polar Lipids (Birmingham, AL), fatty acids were from Larodan AB (Malmö, Sweden), sphingosylphosphorylcholine was from Matreya Inc. (Pleasant Gap, PA) and cholesterol-d_6 was from Cambridge Isotope Laboratories Inc. (Andover, MA). All solvents were of HPLC or analytical grade and were purchased from Merck or Rathburn Chemicals Ltd. (Walkerburn, Scotland).

Cell Culture. F92-99 control fibroblasts and 93.41 NPC fibroblasts obtained as described (*12*) were cultured in Eagle's minimum essential medium (MEM) supplemented with 10% fetal bovine serum (FBS), 2 mM L-glutamine, 100 IU/mL penicillin, 100 μg/mL streptomycin, and 10 mM Hepes, pH 7.4. Confluent-resting cells representing passages 15−20 were used for virus isolation. Four days after reaching confluence, the cells were defined as confluent resting.

[1] Abbreviations: ESI-MS, electrospray ionization mass spectrometry; GSL, glycosphingolipids; PC, phosphatidylcholine; PE, phosphatidylethanolamine; PS, phosphatidylserine; NPC, Niemann−Pick type C; SM, sphingomyelin; VSV, vesicular stomatitis virus.

Cholesterol Loading of Control Fibroblasts. Control fibroblasts grown in MEM containing 10% FBS were washed with PBS and incubated in the presence or absence of cholesterol/methyl-β-cyclodextrin complexes (prepared as in ref *2*; final sterol concentration 50 μg/mL) in serum-free medium supplemented with 2 μg/mL PKF 058-035. After 1 h of incubation, 5% lipoprotein-deficient serum (*13*) was added, and the cells were further incubated for 7 or 23 h in the continued presence of the cholesterol/cyclodextrin complexes. The cells were washed twice with 0.2% bovine serum albumin containing PBS and three times with PBS, scraped in PBS, and the protein concentration was measured according to the method of Lowry (*14*).

Virus Purification. Confluent flasks of control and NPC fibroblasts were infected with VSV or influenza virus. VSV was grown as described in ref *15*. Influenza stock N virus A/chick/Germany/49/Hav2Neq1 was grown as described previously (*16*). The viruses were adsorbed to cells in infection medium (MEM, 0.2% BSA, 2 mM L-glutamine, 100 IU/mL penicillin, 100 μg/mL streptomycin, and 20 mM Hepes, pH 7.4.), and after 1 h the medium was replaced by fresh infection medium. After 24 h the medium was collected, and the viruses were purified as in ref *9*. For mass spectrometric analyses, the buffer was exchanged by resuspending the purified virus pellet in 10 mM Hepes, pH 7.4, overnight and pelleting through a 50% glycerol/Hepes, pH 7.4, cushion in a Beckman SW60Ti rotor at 83000*g* for 2 h. The purity of virus proteins was analyzed by SDS−polyacrylamide gel electrophoresis and silver staining, and the virus particles were visualized by negative staining electron microscopy. The protein concentration was determined by reacting with fluorescamine (*17*) or according to the method of Lowry (*14*).

Electron Microscopy. Negative staining was carried out using conventional methods. Virus samples were applied to carbon-coated EM grids for 60 s. The excess virus was removed with filter paper, and a drop of 1% potassium phosphotungstate, pH 6.5, was applied to the grid. The reagent was removed after 60 s. The samples were observed in a JEOL JEM EX-1200 electron microscope operated at an acceleration voltage of 60 kV.

Synthesis of Phospholipid Standards. Sphingomyelins with a 14:0, 17:0, 23:0, or 25:0 fatty acid residue were synthesized from sphingosylphosphocholine and the respective fatty acid as described previously (*18*, *19*). The sphingomyelin product was purified using a NH_2-bonded silica cartridge (*20*) followed by reverse-phase HPLC on an Ultrasphere ODS column (Beckmann, 5 μm particle size, 250 × 4.6 mm) eluted with 5% chloroform in methanol at 1 mL/min. Di-21:0-PE and -PS were synthesized from the corresponding PC by using phospholipase D-mediated transesterification (*21*). The products were purified on a Lichrosphere 100 DIOL column (Alltech, 5 μm particle size, 250 × 4.6 mm) using the elution conditions described by others (*22*).

Lipid Extraction. Cellular lipids were extracted as described (*23*). Extractions were performed in silylated screw-cap vials (Alltech, Deerfield, IL**)** to avoid losses due to adsorption to glass. For the quantification of the cellular phospholipid species by ESI-MS, the membrane extracts were spiked with the following mixture of internal standards dissolved in chloroform/methanol (C/M 1:2): 14:1/14:1-PC, 20:1/20:1-PC, 22:1/22:1-PC, 14:0-SM, 17:0-SM, 23:0-SM,

25:0-SM, 14:1/14:1-PE, 20:1/20:1-PE, 22:1/22:1-PE, 14:1/14:1-PS, 20:1/20:1-PS, and 22:1/22:1-PS (*11*). For the quantification of cholesterol the extract was spiked with cholesterol-d_6 as an internal standard.

Determination of Total Glycosphingolipid Content. To assess the total cellular sphingolipid concentration, aliquots of the lipid extract were subjected to acid hydrolysis, and the released sphingosine was determined by a fluorometric method (*24*), using a Hitachi F-4000 spectrofluorometer. Bovine brain sphingomyelin was used as the standard. To obtain the concentration of glycosphingolipids, the concentration of sphingomyelin, determined by MS, was subtracted. No correction was done for free sphingosine or ceramide as their concentrations in fibroblasts are negligible as compared to that of glycosphingolipids (*25*, *26*).

Electrospray Ionization Mass Spectrometry. ESI-MS analysis of phospholipids was carried out with a triple quadrupole instrument (Perkin-Elmer Sciex API 300, Ontario, CA) in the positive ion mode. The lipids dissolved in chloroform/methanol (C/M), 1:2, containing 1% NH_4OH were infused to the electrospray source at a flow rate of 2.5−5 μL/min. The phospholipid species were identified on the basis of (i) their characteristic *m*/*z* value, (ii) precursor ion or neutral loss scans, and (iii) acid sensitivity of the alkenyl species. Since the instrument response can vary strongly depending on the phospholipid acyl chain length and unsaturation (*11*), several internal standards were included (see above). For other details including data analysis, see ref *11*. All of the phospholipids were analyzed in the positive ion mode with PE and PS giving their characteristic neutral losses of 141 and 185, respectively, and PC and SM precursors of 184. It should be noted that the neutral loss 141 for PE gives a lower response for plasmalogen species than for diacyl species as shown previously (*10*). Therefore, this method leads to an underestimation of the total PE content. Cholesterol was quantified with an Esquire-LC ion-trap instrument (Bruker-Franzen Analytik, Bremen, Germany) after sulfation in the presence of cholesterol-d_6 internal standard (*27*). Nitrogen was used as the nebulizing (at 5−6 psi) and the drying gas (5−7 L/min at 200 °C). The potentials of the spray needle, capillary exit, and skimmer 1 were set to ±4000, 90−150, and 25−50 V, respectively. For each spectrum 100 scans were averaged.

RESULTS

Lipid Composition of Normal and NPC Human Fibroblasts. The NPC disease is caused by mutations in either of two recently identified genes, NPC1 or NPC2 (*28*, *29*), the precise functions of which remain unknown. At the cellular level, the disease is manifested by massive accumulation of free cholesterol in late endocytic organelles (*30*). For the present study, we chose a NPC primary fibroblast line (93.41) that has previously been used in cell biological and biochemical analyses (*12*, *31*−*33*). These cells lack detectable NPC1 protein (*31*) and are characterized by lysosomal deposition of unesterified cholesterol both biochemically and morphologically. Quantitative determination of the major lipid classes in a confluent culture of the NPC fibroblasts and control fibroblasts was carried out, and the results are shown in Figure 1. The major difference between the two cell lines was an ~2.5-fold higher content of free cholesterol in the patient cells (Figure 1A). This corresponds to

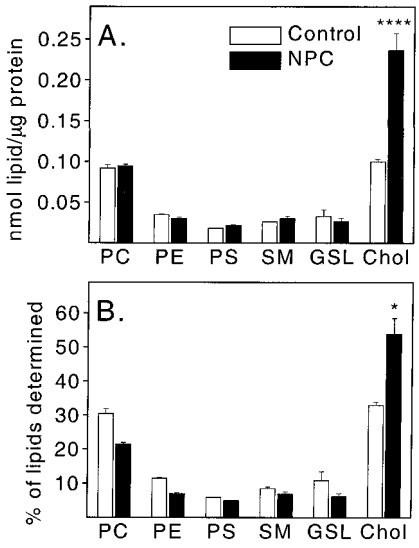

FIGURE 1: Total lipid composition of control and NPC 93.41 fibroblasts. Phospholipid and cholesterol quantification was performed by ESI-MS, and glycosphingolipids (GSL) were quantified by determining the amount of free sphingosine base after acid hydrolysis as detailed in Experimental Procedures. Lipid concentrations are expressed as nmol of lipid/μg of protein (A) and as mol % of all the lipid classes determined (B). Error bars = SEM (n = 3−12). **** = $p < 0.001$ and * = $p < 0.05$ between control and NPC (Student's *t*-test). Note that the amount of PE is probably underestimated due to the lower detection sensitivity of plasmalogens (see Experimental Procedures) that have been reported to represent ~50% of fibroblast PE (*62*).

cholesterol representing about 50% of total lipids determined in NPC cells and 30% of lipids in control cells (Figure 1B). In contrast, the contents of the major glycerophospholipids phosphatidylcholine (PC), phosphatidylethanolamine (PE), and phosphatidylserine (PS) as well as sphingomyelin (SM) and total glycosphingolipid were not statistically different (Figure 1A). The NPC 93.41 cells thus represent a model of a chronically cholesterol-loaded cell type with no major differences in the total levels of polar lipids.

Quantitative ESI-MS analysis of the phospholipid molecular species distribution in normal and NPC fibroblasts is presented in Figure 2. The most abundant PC species in control fibroblasts were 34:1, 36:1, 36:2, and 32:1, while the most abundant PE species were 36:1, 38:4, 36:2, and 34:1. The major PS species was 36:1 followed by 40:5, 40:6, and 38:3. In SM, 16:0 was the most common acyl residue, followed by 24:1, 24:0, and 16:1. Thus, significant differences in the acyl chain saturation levels between glycerophospholipid classes were observed, with PC having the highest degree of saturation (10% saturated, 40% monounsaturated, and 25% polyunsaturated species in control cells) and PE the highest degree of unsaturation (1% saturated, 24% monounsaturated, and 56% polyunsaturated species in control cells) (see Table 1). These data agree well with what is known about the degree of unsaturation of different phospholipid classes in mammalian cells, e.g., that PC is usually rich in monounsaturates, PE in polyunsaturates (*34*, *35*), and SM in saturates (*36*).

In general, the phospholipid molecular species compositions of control and NPC cells were closely similar. For instance, no statistically significant differences were found in the total cellular PS or SM acyl species in NPC compared to control (Figure 2C,D). However, in the case of NPC cell

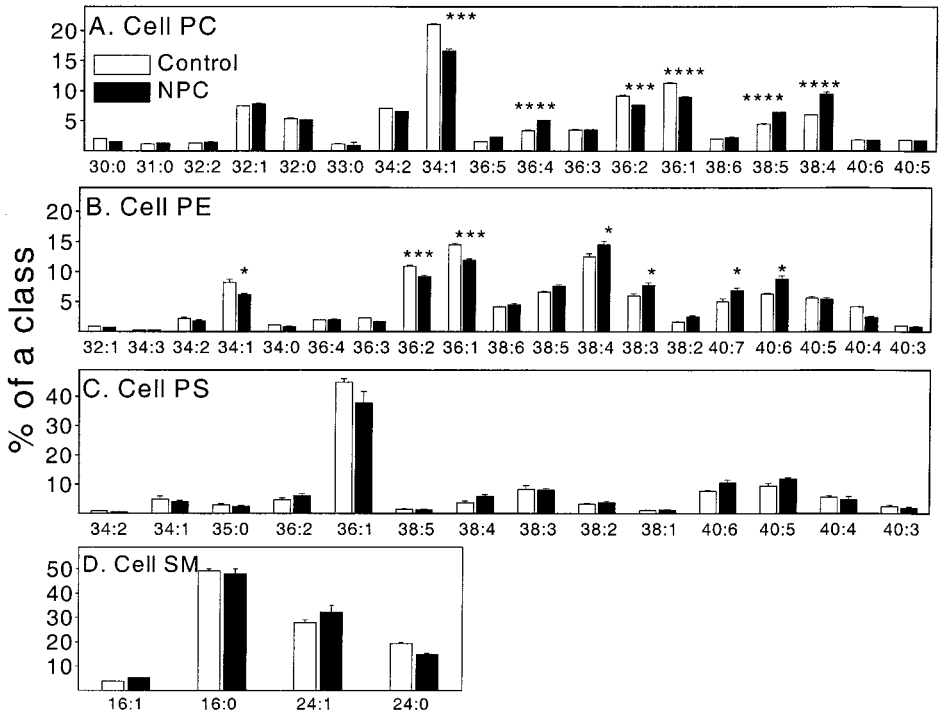

FIGURE 2: Molecular species composition of phospholipid classes in control and NPC fibroblasts as determined by ESI-MS. The individual molecular species were quantified as indicated in Experimental Procedures using internal standards. The molecular species are identified on the basis of the total number of carbons and double bonds in the acyl chains. The MS method used does not allow identification of the individual acyl residues. In case of SM, the length and unsaturation of the single acyl residue are indicated, and its identity is based on the assumption that each species contains the normal sphingosine base. PC (A), PE (B), PS (C), and SM species (D). Error bars = SEM ($n = 3-4$). **** = $p < 0.001$, *** = $p < 0.005$, and * = $p < 0.05$ between control and NPC. The following minor molecular species with *m/z* values corresponding to either diacyl or alkenylacyl/alkylacyl species have been omitted from the figure for clarity and because their concentrations did not vary significantly between control and NPC samples. PC: diacyl 33:2/alkenyl 34:1/alkyl 34:2 (*m/z* pos 744); diacyl 33:1/alkenyl 34:0/alkyl 34:1 (*m/z* pos 746); diacyl 35:2/alkenyl 36:1/alkyl 36:2 (*m/z* pos 772); diacyl 35:1/alkenyl 36:0/alkyl 36:1 (*m/z* pos 774). PE: diacyl 33:2/alkenyl 34:1/alkyl 34:2 (*m/z* pos 702); diacyl 33:1/alkenyl 34:0/alkyl 34:1 (*m/z* pos 704); diacyl 35:2/alkenyl 36:1/alkyl 36:2 (*m/z* pos 730); diacyl 35:1/alkenyl 36:0/alkyl 36:1 (*m/z* pos 732); diacyl 39:6/alkenyl 40:5/alkyl 40:6 (*m/z* pos 778); diacyl 39:5/alkenyl 40:4/alkyl 40:5 (*m/z* pos 780).

Table 1: Degree of Unsaturation of PC, PE, and PS Diacyl Species in Fibroblasts and Viruses[a]

	% of a class						
	cells		infl virus		VSV		acutely cholesterol-loaded cells
	control	NPC	control	NPC	control	NPC	
PC							
saturates	9.8 (0.19)	8.8 (0.59)	8.6 (0.06)	8.8 (0.11)	13.3 (0.89)	9.7 (0.14)	4.6 (0.22)
monounsaturates	39.9 (0.32)	33.5 (0.26)	50.5 (0.34)	36.9 (0.07)	48.4 (1.13)	38.8 (0.51)	31.4 (0.13)
polyunsaturates	24.8 (0.16)	32.6 (0.52)	14.07 (0.3)	25.2 (0.14)	14.6 (0.46)	21.9 (0.13)	40.5 (1.14)
PE							
saturates	1.1 (0.06)	0.84 (0.13)	nd	nd	nd	nd	1.0 (0.15)
monounsaturates	23.6 (0.85)	18.8 (0.47)	40.8 (0.49)	27.8 (0.24)	37.0 (0.21)	25.8 (0.15)	21.1 (1.87)
polyunsaturates	56.0 (0.50)	62.7 (1.05)	39.4 (1.52)	52.5 (1.26)	43.0 (0.78)	56.2 (1.15)	59.7 (1.59)
PS							
saturates	3.0 (0.43)	2.4 (0.26)	2.8 (0.15)	2.3 (0.13)	2.6 (0.25)	2.3 (0.37)	3.0 (0.25)
monounsaturates	50.7 (2.0)	43.42 (2.2)	47.0 (0.75)	37.8 (0.93)	50.1 (7.21)	35.9 (0.04)	47.4 (0.36)
polyunsaturates	37.7 (0.48)	44.6 (2.3)	41.7 (1.14)	52.7 (0.84)	38.6 (6.33)	51.8 (0.03)	42.1 (1.13)

[a] The values represent average percentages (±SEM) of diacyl species from Figures 2, 5, 6, and 7 grouped according to their degree of unsaturation. nd = not detectable.

derived PC and PE, a decrease in the most abundant mono- and diunsaturated species was observed while some of the long-chain polyunsaturated species were increased (Figure 2A,B).

Lipid Class Analysis of Viruses Budding through the Plasma Membrane. To isolate samples of the plasma membrane, we infected control and NPC fibroblasts with influenza virus or VSV and collected the viruses budded to the medium after 24 h of infection. The viruses were isolated by gradient centrifugation and found to be essentially pure as judged by SDS−PAGE and silver staining (Figure 3A). Furthermore, electron microscopic examination of the viral particles isolated from control and NPC fibroblasts revealed characteristic profiles of both viruses (Figure 3B−E).

We then compared the lipid class distributions of the different viruses with each other and with the cellular lipid profiles. Since the protein−lipid ratios between cells and viruses and between different virus species can be markedly

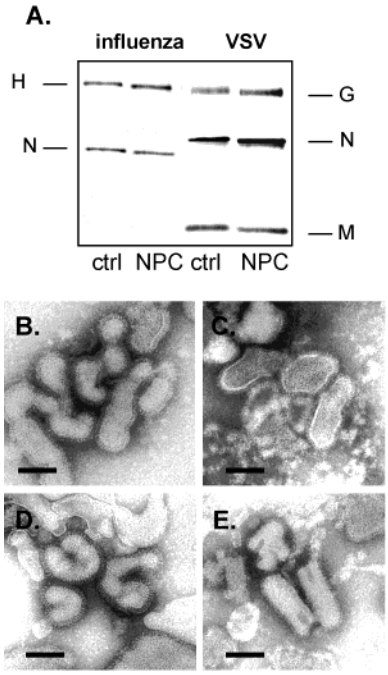

FIGURE 3: Biochemical and morphological analysis of the purity of viruses. Influenza virus and VSV from control and NPC fibroblasts were purified by gradient centrifugation, and an equal amount of protein in each preparation was analyzed by SDS−PAGE and silver staining (A). The viral proteins HA, N, G, and M are indicated. The virus particles were analyzed by negative staining electron microscopy. Control cell derived influenza virus (B), control cell derived VSV (C), NPC cell derived influenza virus (D), and NPC cell derived VSV (E). Bar = 100 nm.

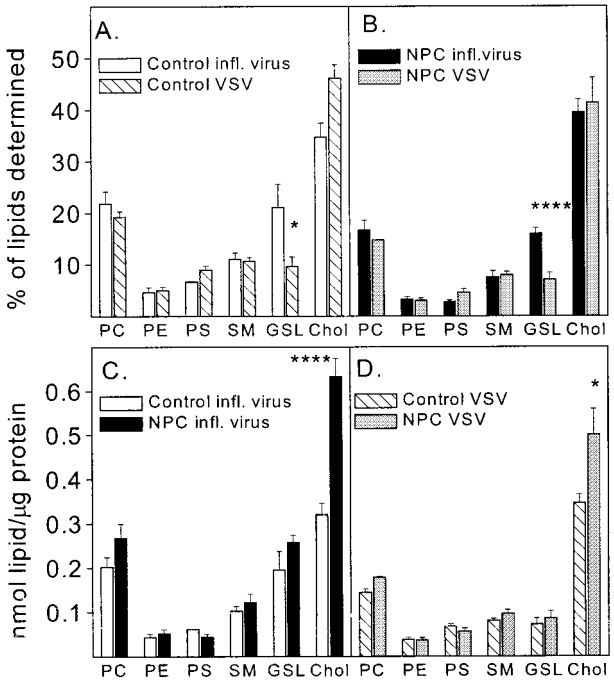

FIGURE 4: Lipid class composition of influenza virus and VSV grown in control or NPC fibroblasts. The lipid classes were quantified as described in Experimental Procedures. Lipid concentrations are expressed as mol % of all the lipid classes determined in control cell derived viruses (A) and NPC cell derived viruses (B) and as nmol of lipid/μg of protein in influenza (C) and VSV (D). Error bars = SEM ($n = 3-12$). * = $p < 0.05$ and **** = $p < 0.001$ between indicated bars. Note that the amount of PE may be underestimated (see legend to Figure 1).

different (*37*), these comparisons are based on data presented as mole percent of all of the lipid classes determined (Figures 4A,B and 1B). To compare the content of lipids in a given virus or the lipid contents between the same virus type derived from control and NPC cells, the data are shown as the amount of lipid (in nanomoles) per the amount of viral protein (Figure 4 C,D).

The most striking difference between the lipid composition of control cell derived influenza and vesicular stomatitis viruses was a 2−3-fold enrichment of glycosphingolipids in the influenza virus envelope (Figure 4A). The fraction of glycosphingolipids among VSV lipids was about the same as that in the total cell (compare Figures 4A and 1B). Notably, compared to the whole cell, cholesterol was relatively enriched in the viruses, in particular VSV (Figure 4 vs Figure 1B). This agrees with the established enrichment of cholesterol in the plasma membrane (*38*, *39*). The molar ratio of cholesterol:glycosphingolipid was ~1:0.6 in the influenza virus originating from control cells (Figure 4C) whereas it was ~1:0.2 in the control cell derived VSV (Figure 4D).

A similar enrichment of glycosphingolipids in influenza virus was also found for the NPC cell derived viruses (Figure 4B). When the lipid content of the NPC and control cell derived viruses was compared, we found a significant enrichment of cholesterol in both influenza virus and VSV budded through the NPC fibroblast plasma membrane (Figure 4C,D). The NPC influenza virus envelope contained about twice as much cholesterol as the control influenza virus (Figure 4C), whereas in NPC VSV the enrichment was more moderate, about 1.4-fold (Figure 4D). No significant differences in the other lipid classes were observed, in line with the results from the whole cells (Figure 1A).

Phospholipid Molecular Species Composition of the Viruses. We next analyzed the phospholipid molecular species profiles of the two virus species derived from control and NPC cells. These data are presented in Figures 5 and 6 and Table 1. When comparing the unsaturation of control cell derived viral phospholipids and cellular phospholipids, we found that polyunsaturated species of both PC and PE were depleted from the viruses compared to the cell. In influenza virus 14% of PC and in VSV 15% of PC were polyunsaturated vs 25% in the cell. In PE, 39% and 43% of the species were polyunsaturated in influenza virus and VSV, respectively, compared to 56% of cellular PE (see Table 1). For PS and SM, no significant differences in the acyl chain saturation between the host and viral phospholipids were found (Table 1, Figure 6C,D vs Figure 2D). These data are in accordance with the reported enrichment of more saturated lipid species in the plasma membrane (*40*, *41*).

When the phospholipid species composition of the two control cell derived viruses was compared, we found, somewhat surprisingly, that the influenza and VSV phospholipid species composition was very closely similar (Figures 5 and 6). Comparison of the phospholipid molecular species profiles of control and NPC cell derived viruses revealed, however, significant differences. Both the influenza and VSV from NPC cells contained more polyunsaturated phospholipids than the corresponding control viruses (Figures 5 and 6, Table 1). In influenza PE, there was an ~30% reduction in the monounsaturated species with short acyl

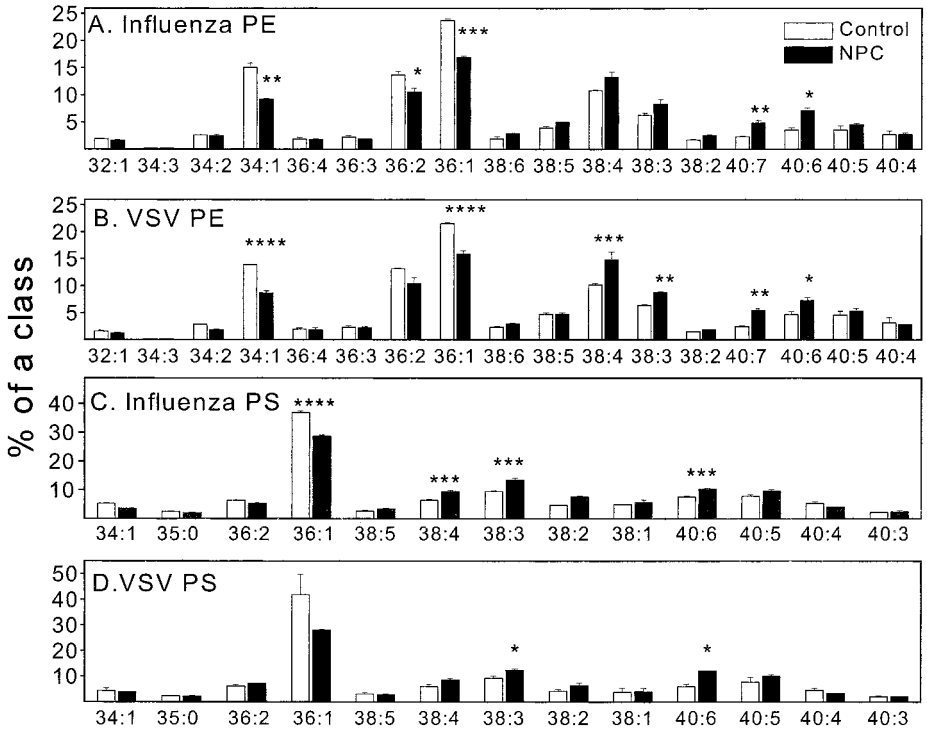

FIGURE 5: Molecular species composition of PE and PS from influenza virus and VSV grown in control or NPC fibroblasts. The individual molecular species were quantified as indicated in Experimental Procedures using internal standards. PE molecular species in influenza (A) and VSV (B) and PS species in influenza (C) and VSV (D). Error bars = SEM ($n = 4-6$). **** = $p < 0.001$, *** = $p < 0.005$, ** = $p < 0.01$, and * = $p < 0.05$ between values for control and NPC. The minor PE molecular species indicated in the legend of Figure 2 have been omitted from panels A and B for clarity because their concentrations did not vary between NPC and control samples.

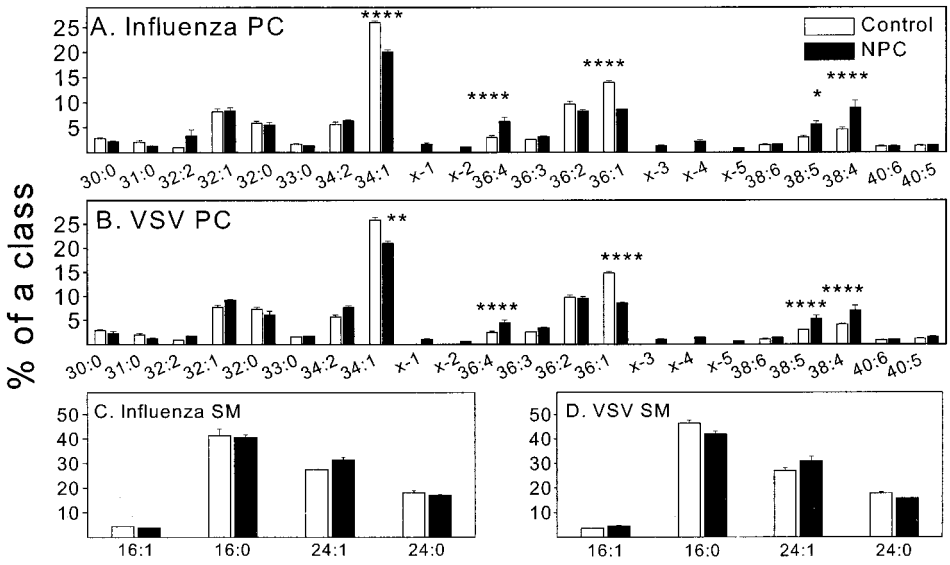

FIGURE 6: Molecular species composition of PC and SM from influenza virus and VSV grown in control or NPC fibroblasts. Molecular species for PC in influenza virus (A) and VSV (B) and SM in influenza virus (C) and VSV (D). Error bars = SEM ($n = 4-6$). **** = $p < 0.001$, ** = $p < 0.01$, and * = $p < 0.05$ between values for control and NPC. The minor PC species indicated in the legend of Figure 2 have been omitted from panels A and B for clarity because their concentrations did not vary significantly between NPC and control samples. Some minor polyunsaturated diacyl/alkylacyl/alkenylacyl PC species, however, were only detectable in viruses from NPC cells and are designated as follows: x-1, diacyl 35:5/alkenyl 36:4/alkyl 36:5 (*m/z* pos 766); x-2, diacyl 35:4/alkenyl 36:3/alkyl 36:4 (*m/z* pos 768); x-3, diacyl 37:6/alkenyl 38:5/alkyl 38:6 (*m/z* pos 792); x-4, diacyl 37:5/alkenyl 38:4/alkyl 38:5 (*m/z* pos 794); x-5, diacyl 37:4/alkenyl 38:3/alkyl 38:4 (*m/z* pos 796).

chains (typically C32−36) and a corresponding increase in the polyunsaturated species with longer chains (C38−40) in the NPC derived virus compared to control cell derived virus (Figure 5A). The increase was most striking for the PE molecules containing the highest number of double bonds, as exemplified by the doubling of the proportion of PE, 40:7 and 40:6. A similar increase in the unsaturation and, consequently, in chain length of PE was observed in the NPC cell derived VSV when compared to control VSV (Figure 5B). Furthermore, the same tendency was evident for both PS and PC from NPC cell derived viruses (Figures 5C,D and 6A,B, Table 1). However, in the case of SM, the

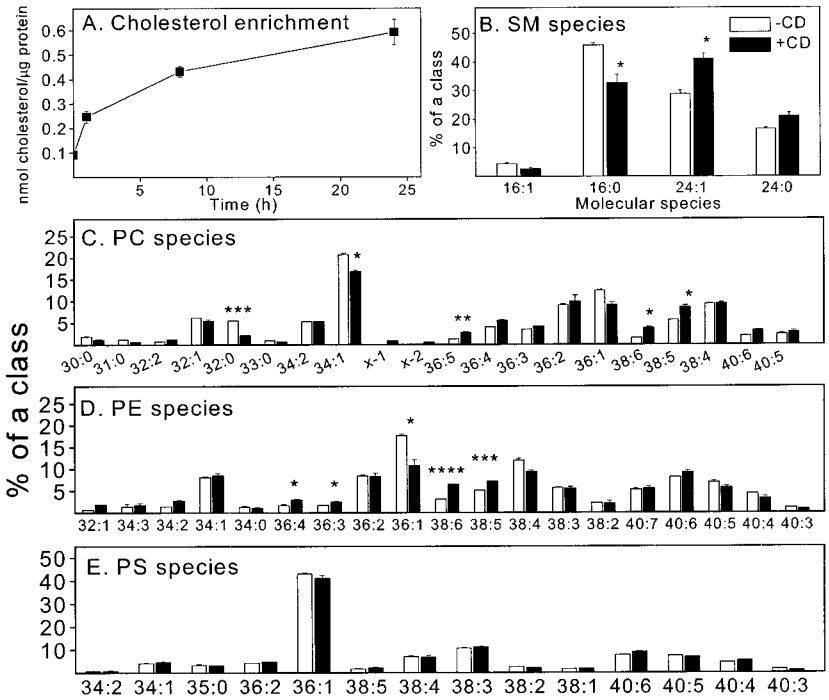

FIGURE 7: Cholesterol loading of normal fibroblasts using methyl-β-cyclodextrin/cholesterol complexes and its effect on phospholipid molecular species composition. Cholesterol enrichment in fibroblasts loaded for 0, 1, 8, and 24 h with cyclodextrin/cholesterol complexes (A). Molecular species composition of individual SM (B), PC (C), PE (D), and PS (E) species in nonloaded (−CD) and loaded (+CD) fibroblasts. **** = $p < 0.001$, *** = $p < 0.005$, ** = $p < 0.01$, and * = $p < 0.05$ between values for nonloaded and loaded cells. Error bars = SEM ($n = 3$). The minor PC and PE species indicated in the legend of Figure 2 have been omitted as there were no differences in their concentrations between the samples. Some minor polyunsaturated diacyl/alkylacyl/alkenylacyl PC species were, however, only detectable in loaded cells and are designated with the following numbers in the figure: x-1, diacyl 35:5/alkenyl 36:4/alkyl 36:5 (*m/z* pos 766); x-2, diacyl 35:4/alkenyl 36:3/alkyl 36:4 (*m/z* pos 768).

difference between NPC and control cell derived species was negligible in both viruses (Figure 6C,D).

Also, Acute Cholesterol Loading Increases Phospholipid Acyl Chain Unsaturation. To test whether the shift in acyl chain saturation observed between normal and NPC fibroblasts is a phenomenon related only to the mutant phenotype or represents a more general response to cholesterol accumulation, we loaded normal fibroblasts acutely with cholesterol using cholesterol/cyclodextrin complexes as cholesterol donors (*2*). An inhibitor of cholesterol esterification (PKF 058-035) was included in some incubations to prevent cellular homeostatic responses from diminishing the free cholesterol content of membranes. In agreement with previous studies (*2*, *42*), we found that the cholesterol loading was relatively fast and efficient, with a 2-fold increase in 1 h and a 5-fold increase in 24 h (Figure 7A. Moreover, quantification of the PC, PE, PS, and SM classes after 24 h of loading showed that the most significant change was the increase of PC by 20−30% in the cholesterol-loaded cells (data not shown). This is in line with a previous study (*2*).

ESI-MS analysis of the phospholipid molecular species composition was performed on cells loaded with cholesterol for 8 or 24 h. Marked changes in the acyl chain length and saturation degrees of SM, PC, and PE were found after 24 h of loading. In SM, the normally most abundant species, 16:0, was decreased by ∼30%, and the longest unsaturated species, 24:1, was correspondingly increased, now being the most abundant species (Figure 7B). The fully saturated PC species (32:0) decreased by ∼50%, the monounsaturated species by ∼20%, and the polyunsaturated species were correspondingly increased (Figure 7C and Table 1). There were also significant changes in the molecular species profile of PE, i.e., an ∼10% decrease in monounsaturated and a similar increase in polyunsaturated species (Figure 7D and Table 1). In PS, the changes were negligible (Figure 7D).

Notably, the tendency toward increased unsaturation of select phospholipids was observed already after 8 h of cholesterol loading. For PC, significant increases in the molecular species 36:5, 38:6, 38:5, and 40:6 were observed at this time (data not shown). However, in PE and SM the differences seemed to develop more slowly as they were not detectable after 8 h of loading. To test whether the increase in polyunsaturated acyl species in cholesterol-loaded cells was dependent on blocking cholesterol esterification, the loading was performed in the absence of the esterification inhibitor. Under these conditions, a 45% decrease in saturated, a 20% decrease in monounsaturated, and a complementary 33% increase in polyunsaturated PC species after 24 h of loading was observed (data not shown). Thus, similar changes in acyl chain saturation were observed also when cholesterol esterification was not inhibited.

DISCUSSION

In this study, we used the high-resolution ESI-MS method to analyze the lipid profiles of normal and cholesterol-loaded cells, particularly their plasma membrane. The analysis was focused on the plasma membrane lipid composition for the following reasons. First, there is increasing evidence for the existence of specialized lipid domains in the plasma membrane although their actual composition has not been defined. Second, it is not known whether the plasma membrane lipid

composition of NPC cells, characterized by cellular cholesterol deposition, differs from normal. Third, changes in plasma membrane lipid composition could have important functional consequences, e.g., on membrane trafficking or the exchange of signals with the extracellular environment. To obtain preparations enriched in plasma membrane lipids, we isolated enveloped viruses budding through this membrane. The advantage of this method is that the viruses can be easily separated from the host cells with minimal contamination. However, it cannot be excluded that the lipid composition may be biased, e.g., due to selective sampling of lipids by the viral proteins (*37*, *43*).

Comparison of VSV and Influenza Virus Lipids. Previous studies have indicated that influenza virus selects more ordered, raft-like domains for budding, while VSV buds from raft-depleted membranes (*9*, *44*). The most notable difference between the VSV and influenza virus lipid compositions determined in the present study was a clear enrichment of glycosphingolipids in the influenza virus. This fits with the hypothesis that influenza virus buds from rafts, i.e., domains enriched in glycosphingolipids.

Saturated phospholipids along with sphingolipids are known to promote the formation of an ordered membrane phase (*45*, *46*). Therefore, more highly saturated phospholipids might be expected to enrich in influenza virus (*9*). However, we found that the phospholipid acyl chain composition of influenza virus was quite similar to that of VSV. It is possible that compositional differences between domains employed by budding viruses and potentially existing in uninfected cells were masked by cytopathic effects of the infection. An infection time of 24 h was used in order to collect sufficient material for the analyses. This was considered warranted because the differences in detergent solubility, cyclodextrin-mediated efflux of cholesterol, and fluorescence polarization between influenza and VSV were observed after such a long infection of BHK cells (*9*). On the other hand, a long infection time has been shown to abolish the apical/basolateral polarity in Madin−Darby canine kidney epithelial cells with concomitant loss of lipid compositional differences between influenza and VSV (*47*). In any case, on the basis of our data on fibroblast-derived viruses, it seems likely that the enrichment of glycosphingolipids in influenza virus may be one of the determinants responsible for the observed differences between the BHK cell derived viruses (*9*). Moreover, if the viral infection indeed undermines some of the lipid compositional differences, the enrichment of glycosphingolipids to rafts could be even more pronounced than what is suggested by the present data.

Lipid Composition of NPC Membranes. The most significant alterations in the plasma membrane lipid composition of NPC cells were the increased cholesterol content and the increased proportion of polyunsaturated glycerophospholipid species. The latter finding accords with the reported high phospholipid acyl chain unsaturation in several tissues of the NPC mouse (*48*). In another study, an increase in the ratio of saturated to unsaturated fatty acids and a decrease in monounsaturated fatty acids in NPC fibroblasts were reported (*49*). However, it appears that also in this case the polyunsaturated species were actually increased.

On the basis of the resistance of the disease cells to the fungal sterol-binding antibiotics filipin and amphotericin B, the NPC plasma membrane has been considered to be cholesterol depleted (*49*, *50*). On the other hand, calculations based on the extractability of radiolabeled cholesterol by cyclodextrin have suggested that the cholesterol content of the plasma membrane is normal (*31*). The present virus data indicate that the plasma membrane of NPC cells may contain more cholesterol than that of normal cells. This could be related to the increased cholesterol synthesis and/or "spilling over" of the excess cholesterol from the endocytic organelles to the plasma membrane.

The resistance of NPC cells to polyene antibiotics may thus not indicate a reduced membrane sterol content but rather be associated with altered lipid organization, as demonstrated for mutant, amphotericin B resistant Chinese hamster ovary cells (*51*). Furthermore, susceptibility to the polyene antibiotic may not reflect the plasma membrane lipid organization alone, since amphotericin B and nystatin cause caveolar endocytosis and formation of abnormally large endocytic structures (*52*). Amphotericin B seems to be rapidly internalized in fibroblasts because it induces the fragmentation of lysosomes within 30−60 min (our unpublished observations).

Membrane Cholesterol Content and Phospholipid Fatty Acyl Chain Structure. An intriguing principle emerging from our study is the modulation of phospholipid acyl chain composition toward increasingly polyunsaturated species upon increasing membrane cholesterol content. In NPC cells, this phenomenon could be due to secondary metabolic effects rather than being directly caused by the excessive membrane cholesterol. For instance, β-oxidation of polyunsaturated fatty acids could be impaired due to the peroxisomal dysfunction (*53*, *54*). However, cholesterol loading of normal cells also induced an increase of polyunsaturated phospholipid species, particularly in PC. An increased concentration of polyunsaturates thus seems to reflect a true regulatory response to cholesterol increase. Interestingly, the changes were more pronounced in the purified plasma membrane preparations than in whole cells, presumably because of the enrichment of cholesterol in the plasma membrane. In NPC cells, increased acyl chain unsaturation was observed for all the glycerophospholipids studied but not for SM, while in normal cells acutely loaded with cholesterol an increase in unsaturation was seen most clearly for SM and PC. These two lipid classes are located in the outer leaflet of the plasma membrane that presumably initially receives the bulk of the cholesterol load. Moreover, the levels of both PC and SM are closely coupled to cellular cholesterol homeostasis. The biosynthesis of PC is activated upon cholesterol loading of fibroblasts or macrophages (*2*, *55*) while hydrolysis of plasma membrane sphingomyelin leads to reduction of free cholesterol via its esterification (*56*, *57*). Although the reason for the lack of SM modification in NPC remains elusive, a fraction of the SM pool may be sequestered in lysosomes and thus removed from regulatory circuits capable of responding to the cholesterol excess elsewhere in the cell.

The direct relationship between cellular cholesterol content and phospholipid saturation level has only been addressed in few studies, and the phenomenon observed in the present work has, to our knowledge, not been reported earlier. In one study, marked alterations in eukaryotic membrane sterol composition were found to be insufficient to change total phospholipid head or acyl group composition (*58*), but only

fully saturated and monounsaturated species were analyzed. On the other hand, studying sterol auxotrophic cells, Freter et al. (*59*) did find a correlation between the membrane cholesterol content and fatty acid composition. Sterol depletion was found to associate with a reduction in the relative amount of phospholipids containing saturated acyl chains. Extrapolating from our data, the expected effect would be opposite. However, the experimental systems studied were quite different, and it is not obvious that cholesterol depletion and loading should have antagonistic effects.

We propose that the increase in polyunsaturated phospholipid species in response to cholesterol loading may serve as a protective mechanism counteracting the membrane rigidifying effect of cholesterol. This mechanism is likely to operate in parallel with compensatory systems aiming at lowering the membrane cholesterol content (e.g., downregulation of LDL receptors and cholesterol biosynthesis, increase of cholesterol esterification). Model membranes rich in polyunsaturated phospholipid species are known to be less susceptible for the stiffening effect of cholesterol than those rich in monounsatured species (*60*). Thus, an increase in polyunsaturated species at the expense of monounsatured ones may help to maintain adequate membrane fluidity in the presence of excess cholesterol. Importantly, this modulating effect may not be observed if only mono/diunsaturated species are analyzed. The mechanisms by which the increased cholesterol content of the membrane induces the phospholipid changes remain to be elucidated. One possibility is that the excess of cholesterol (or its metabolite) enhances the synthesis of polyunsaturated fatty acids by upregulating certain fatty acid desaturases, such as stearoyl-CoA desaturase (*4*). However, upregulation of this enzyme is not sufficient to explain the present findings since also those polyunsaturated fatty acids that are not derived from stearate, but from essential fatty acids, were increased. Furthermore, in a recent report cholesterol was actually found to repress the transcription of this enzyme (*61*). More likely, mechanisms that do not require de novo fatty acid synthesis could be involved. For instance, cholesterol could enhance the preferential release of polyunsaturated fatty acids from cellular neutral lipids or stimulate their uptake from the medium. Alternatively, the fatty acid preference of enzyme(s) involved in the reacylation of phospholipids might be regulated by cholesterol.

ACKNOWLEDGMENT

We thank Birgitta Rantala for skillful technical assistance.

REFERENCES

1. Brown, M. S., and Goldstein, J. L. (1999) *Proc. Natl. Acad. Sci. U.S.A. 96*, 11041−11048.
2. Leppimaki, P., Mattinen, J., and Slotte, J. P. (2000) *Eur. J. Biochem. 267*, 6385−6394.
3. Leppimaki, P., Kronqvist, R., and Slotte, J. P. (1998) *Biochem. J. 335*, 285−291.
4. Ntambi, J. M. (1999) *J. Lipid Res. 40*, 1549−1558.
5. Simons, K., and Ikonen, E. (1997) *Nature 387*, 569−572.
6. Anderson, R. G. W. (1998) *Annu. Rev. Biochem. 67*, 199−225.
7. Brown, D. A., and London, E. (1998) *Annu. Rev. Cell Dev. Biol. 14*, 111−136.
8. Ikonen, E. (2001) *Curr. Opin. Cell Biol. 13*, 470−477.
9. Scheiffele, P., Rietveld, A., Wilk, T., and Simons, K. (1999) *J. Biol. Chem. 274*, 2038−2044.
10. Brugger, B., Erben, G., Sandhoff, R., Wieland, F. T., and Lehmann, W. D. (1997) *Proc. Natl. Acad. Sci. U.S.A. 94*, 2339−2344.
11. Koivusalo, M., Haimi, P., Heikinheimo, L., Kostiainen, R., and Somerharju, P. (2001) *J. Lipid Res. 42*, 663−672.
12. Hölttä-Vuori, M., Määttä, J., Ullrich, O., Kuismanen, E., and Ikonen, E. (2000) *Curr. Biol. 10*, 95−98.
13. Goldstein, J. L., Basu, S. K., and Brown, M. S. (1983) *Methods Enzymol. 98*, 241−260.
14. Lowry, O. H., Rosebrough, N. J., Farr, A. L., and Randall, R. J. (1951) *J. Biol. Chem. 193*, 265−275.
15. Bennett, M., Wandinger-Ness, A., and Simons, K. (1988) *EMBO J. 7*, 4075−4085.
16. Matlin, K. S., and Simons, K. (1983) *Cell 34*, 233−243.
17. Storrie, B., and Madden, E. A. (1990) *Methods Enzymol. 182*, 203−25.
18. Cohen, R., Barenholz, Y., Gatt, S., and Dagan, A. (1984) *Chem. Phys. Lipids 35*, 371−384.
19. Ramstedt, B., and Slotte, J. P. (1999) *Biophys. J. 76*, 908−915.
20. Kaluzny, M. A., Duncan, L. A., Merritt, M. V., and Epps, D. E. (1985) *J. Lipid Res. 26*, 135−140.
21. Kasurinen, J., and Somerharju, P. (1995) *Biochemistry 34*, 2049−2057.
22. Silversand, C., and Haux, C. (1997) *J. Chromatogr., B: Biomed. Sci. Appl. 703*, 7−14.
23. Folch, J. M., Lees, M., and Sloane-Stanley, G. H. (1957) *J. Biol. Chem. 226*, 497−509.
24. Naoi, M., Lee, Y. C., and Roseman, S. (1974) *Anal. Biochem. 58*, 571−577.
25. Mano, N., Oda, Y., Yamada, K., Asakawa, N., and Katayama, K. (1997) *Anal. Biochem. 244*, 291−300.
26. Liebisch, G., Drobnik, W., Reil, M., Trumbach, B., Arnecke, R., Olgemoller, B., Roscher, A., and Schmitz, G. (1999) *J. Lipid Res. 40*, 1539−1546.
27. Sandhoff, R., Brugger, B., Jeckel, D., Lehmann, W. D., and Wieland, F. T. (1999) *J. Lipid Res. 40*, 126−132.
28. Carstea, E. D., Morris, J. A., Coleman, K. G., Loftus, S. K., Zhang, D., Cummings, C., Gu, J., Rosenfeld, M., Pavan, W. J., Krizman, D. B., Nagle, J., Polymeropoulos, M. H., Sturley, S. L., Ioannou, Y. A., Higgins, M. E., Comly, M., Cooney, A., Brown, A., Kaneski, C. R., Blanchette-Mackie, E. J., Dwyer, N. K., Neufeld, E. B., Chang, T.-Y., Liscum, L., Straus, J. F., III, Ohno, K., Zeigler, M., Carmi, R., Sokol, J., Markie, D., O'Neill, R. R., van Diggelen, O. P., Elleder, M., Patterson, M. C., Brady, R. O., Vanier, M. T., Pentchev, P. G., and Tagle, D. A. (1997) *Science 277*, 228−231.
29. Naureckiene, S., Sleat, D. E., Lackland, H., Fensom, A., Vanier, M. T., Wattiaux, R., Jadot, M., and Lobel, P. (2000) *Science 290*, 2298−2301.
30. Pentchev, P. G., Vanier, M. T., Suzuki, K., and Patterson, M. C. (1995) in *The metabolic and molecular basis of inherited disease* (Scriver, S. R., Beaudet, A. L., Sly, W. S., and Valle, D., Eds.) pp 2625−2639, McGraw-Hill, New York.
31. Lange, Y., Ye, J., Rigney, M., and Steck, T. (2000) *J. Biol. Chem. 275*, 17468−17475.
32. Lusa, S., Blom, T. S., Eskelinen, E.-L., Kuismanen, E., Månsson, J.-E., Simons, K., and Ikonen, E. (2001) *J. Cell Sci. 114*, 1893−1900.
33. Zhang, M., Dwyer, N. K., Neufeld, E. B., Love, D. C., Cooney, A., Comly, M., Patel, S., Wateri, H., Strauss, J. F., III, Pentchev, P. G., Hanover, J. A., and Blanchette-Mackie, E. J. (2001) *J. Biol. Chem. 276*, 3417−3425.
34. Mahadevappa, V. G., and Holub, B. J. (1982) *Biochim. Biophys. Acta 713*, 73−79.
35. Murphy, E. J., Anderson, D. K., and Horrocks, L. A. (1993) *J. Neurosci. Res. 34*, 472−477.
36. Barenholz, Y., and Thompson, T. E. (1980) *Biochim. Biophys. Acta 604*, 129−158.
37. Lenard, J., and Compans, R. W. (1974) *Biochim. Biophys. Acta 344*, 51−94.

38. Lange, Y., Swaisgood, M. H., Ramos, B. V., and Steck, T. L. (1989) *J. Biol. Chem. 264*, 3786−3793.
39. van Meer, G. (1989) *Annu. Rev. Cell Biol. 5*, 247−275.
40. Renkonen, O., Kääriäinen, L., Simons, K., and Gahmberg, C. G. (1971) *Virology 46*, 318−326.
41. Schneiter, R., Brugger, B., Sandhoff, R., Zellnig, G., Leber, A., Lampl, M., Athenstaedt, K., Hrastnik, C., Eder, S., Daum, G., Paltauf, F., Wieland, F. T., and Kohlwein, S. D. (1999) *J. Cell Biol. 146*, 741−754.
42. Christian, A. E., Haynes, M. P., Phillips, M. C., and Rothblat, G. H. (1997) *J. Lipid Res. 38*, 2264−2272.
43. Pessin, J. E., and Glaser, M. (1980) *J. Biol. Chem. 255*, 9044−9050.
44. Keller, P., and Simons, K. (1998) *J. Cell Biol. 140*, 1357−1367.
45. Schroeder, R., London, E., and Brown, D. (1994) *Proc. Natl. Acad. Sci. U.S.A. 91*, 12130−12134.
46. Schroeder, R., Ahmed, S. N., Zhu, Y., London, E., and Brown, D. A. (1998) *J. Biol. Chem. 273*, 1150−1157.
47. van Meer, G., and Simons, K. (1982) *EMBO J. 1*, 847−852.
48. Nakashima, S., Nagata, K., Banno, Y., Sakiyama, T., Kitagawa, T., Miyawaki, S., and Nozawa, Y. (1984) *J. Lipid Res. 25*, 219−227.
49. Koike, T., Ishida, G., Taniguchi, M., Higaki, K., Ayaki, Y., Saito, M., Sakakihara, Y., Iwamori, M., and Ohno, K. (1998) *Biochim. Biophys. Acta 1406*, 327−335.
50. Dahl, N. K., Reed, K. L., Daunais, M. A., Faust, J. R., and Liscum, L. (1992) *J. Biol. Chem. 267*, 4889−4896.
51. Jacobs, N. L., Andemariam, B., Underwood, K. W., Panchalingam, K., Sternberg, D., Kielian, M., and Liscum, L. (1997) *J. Lipid Res. 38*, 1973−1987.
52. Carozzi, A. J., Ikonen, E., Lindsay, M. R., and Parton, R. G. (2000) *Traffic 1*, 326−341.
53. Schedin, S., Sindelar, P. J., Pentchev, P. G., Brunk, U., and Dallner, G. (1997) *J. Biol. Chem. 272*, 6245−6251.
54. Sequeira, J. S. S., Vellodi, A., Vanier, M. T., and Clayton, P. T. (1998) *J. Inherited Metab. Dis. 21*, 149−154.
55. Tabas, I. (2000) *Biochim. Biophys. Acta 1529*, 164−174.
56. Slotte, J. P. (1999) *Chem. Phys. Lipids 102*, 13−27.
57. Ridgway, N. D. (2000) *Biochim. Biophys. Acta 1484*, 129−141.
58. Silberkang, M., Havel, C. M., Friend, D. S., McCarthy, B. J., and Watson, J. A. (1983) *J. Biol. Chem. 258*, 8503−8511.
59. Freter, C. E., Ladenson, R. C., and Silbert, D. F. (1979) *J. Biol. Chem. 254*, 6909−6916.
60. Huster, D., Arnold, K., and Gawrisch, K. (1998) *Biochemistry 37*, 17299−17308.
61. Bene, H., Lasky, D., and Ntambi, J. M. (2001) *Biochem. Biophys. Res. Commun. 284*, 1194−1198.
62. Heymans, H. S. A., van den Bosch, H., Schutgens, R. B. H., Tegelaers, W. H. H., Walther, J.-U., Hocker-Muller, J., and Borst, P. (1984) *Eur. J. Pediatr. 142*, 10−15.

BI0156714